

First-principles study of water on copper and noble metal (110) surfaces

Jun Ren and Sheng Meng

Department of Physics and School of Engineering and Applied Sciences, Harvard University, Cambridge, Massachusetts 02138, USA
(Received 10 November 2007; revised manuscript received 8 January 2008; published 27 February 2008)

Water structure and dissociation kinetics on a model open metal surface: Cu(110), has been investigated in detail based on first-principles electronic structure calculations. We revealed that in both monomer and overlayer forms, water adsorbs *molecularly*, with a high tendency for diffusion and/or desorption rather than dissociation on clean surfaces at low temperature. Studying water on other noble metal (110) surfaces confirms that Cu(110) is the borderline between intact and dissociative water adsorption, differing in energy by only 0.08 eV. This may lead to promising applications in hydrogen generation and fuel cells.

DOI: [10.1103/PhysRevB.77.054110](https://doi.org/10.1103/PhysRevB.77.054110)

PACS number(s): 68.43.Hn, 61.46.-w, 68.43.Bc, 82.30.Fi

I. INTRODUCTION

There has been a persistent drive for cheaper catalysts and a higher efficiency in industrial chemical synthesis, such as ammonia,¹ and in novel energy applications, for instance, hydrogen generation and purification in fuel cells.² One of the good examples is the water-gas-shift reaction ($\text{H}_2\text{O} + \text{CO} = \text{H}_2 + \text{CO}_2$) for pollute removal and mass H_2 production based on Cu catalysts,³ which are significantly less expensive than noble and transition metal catalysts (Pt or Ru). A full account of the involved mechanism has not been possible, but it is suggested that water dissociation is the rate-limiting process.³

This motivated us to study the fundamental interactions involved in water-Cu systems, with an intention to examine Cu as a possible candidate for cheap catalysts. The study of water on metal surfaces has been a focus for more than three decades^{4,5} due to its immense importance and wide applications in catalysis, corrosion, electrolysis, and biotechnologies. However, most studies so far focus on stable closely packed or smooth (001) surfaces, with open and rumpling surfaces such as metal (110) less studied.^{4,5} Recent developments in this area involve research on femtosecond photoelectron dynamics in interface water clusters⁶ and investigations under near-ambient conditions,⁷ whereby Andersson *et al.* found interesting hydroxyl-induced water wetting on metal surfaces. Most properties such as stable species, phases, and kinetics are found in good agreement with those measured under ultrahigh vacuum environment.⁸

Despite intensive studies, the simplest questions concerning interface water structure remain elusive: Are water molecules intact or dissociated? How easily can they be split to generate H_2 (as future fuels)? What is the energy difference? Recently, the general belief that water adsorbs molecularly and forms intact bilayers resembling bulk ice Ih on precious metal surfaces has been challenged from low energy electron diffraction (LEED),⁹ x-ray photoelectron spectroscopy (XPS),¹⁰ and theoretical studies.¹¹ Based on the coplanar geometry of O atoms in LEED and the density functional theory (DFT) calculation, Feibelman proposed a new structural model in which water binds Ru(0001) through intact and partially dissociated water molecules alternatively.¹¹ Later studies argue that water dissociation is an activated process, and assign the dissociated overlayer due to beam damage.^{12,13}

While water/Ru(0001) is still under debate, there are an increasing number of studies of water on Cu(110), another borderline for water dissociation.⁴ On Cu(110), the LEED pattern $c(2 \times 2)$ was commonly observed above water coverage of 0.15 ML (monolayer) (1 ML is defined as one water per surface Cu atom), and was assigned to hydrogen bond network formation¹⁴⁻¹⁷ and/or dissociation by irradiation.¹⁸ Besides, other surface structures including the parallel chains¹⁸ separated by ~ 50 Å, which are assigned to the chains of water hexamers,¹⁹ and a new (7×8) LEED pattern for two-dimensional overlayers²⁰ are also observed very recently. Contradicting results were reported in recent XPS studies: Ammon *et al.* found that partial dissociation of D_2O occurs at 95 K,¹⁷ while Andersson *et al.* found no dissociation below 150 K.²¹ Theoretical calculations involving water on smooth and stepped Cu surfaces²² with or without preadsorbed oxygen^{23,24} suggested that water dissociation might be assisted by the neighboring oxygen atoms. In addition, the atomic structure of H_2O and $\text{OH} + \text{H}_2\text{O}$ layers, such as adsorption site, water orientation, proton transfer, and dynamical aspects, is far from conclusive.

We have suggested the intact bilayer model mainly composed by the H-down bilayer instead of the half-dissociated adlayer for the water monolayer on Cu(110) recently.²⁵ This is followed by an x-ray absorption study, where Schiros *et al.* found that the H-down/H-up ratio is 2:1 in the nondissociated water adlayer in the (7×8) structure.²⁰ In this work, we extend our calculations to include water molecule adsorption on different sites, various monolayer structures with different orientations, and kinetic barriers for water diffusion and dissociation on Cu(110) and other noble metal (110) surfaces. We remind readers to exercise caution when inferring structural information from total energy calculations: the most stable structure may not be present in experiment. For the case we studied here, by carefully comparing calculated energetics, work function, and vibrational spectroscopy with available experiments, we find that water structure in $c(2 \times 2)$ on Cu(110) to be the intact water overlayer in low temperature experiments, although the half-dissociated overlayer is 0.08 eV more favorable. The presence of the lowest-energy half-dissociated structure is blocked by a barrier of ~ 0.57 eV. This middle-sized energy barrier involves multiple proton transfer processes, and can be overcome by heating or beam illumination. This leads to sensitive water dissociation and/or recombination dynamics in favor of fuel cell

applications. Another merit of this system is the fast H diffusion along $[110]$ grooves, facilitating H_2/O_2 separation. Comparisons with other metal (110) surfaces such as Ag, Au, Pd, and Pt, with or without reconstruction, confirm that Cu(110) is the borderline for water molecular and dissociative adsorption with a smallest energy separation.

This paper is organized as follows. After this introduction, the theoretical methods used in this study are given in Sec. II. Then we present in Sec. III our results of water on Cu(110) in two categories: (i) water monomer adsorption and (ii) water monolayers, with focus on possible structures, diffusion, and dissociation. The results are extended to other noble metal (110) surfaces, unreconstructed or reconstructed, including Ag, Au, Pd, and Pt. Finally, some concluding remarks are given in Sec. IV.

II. METHODS

The first-principles calculations were performed with the Vienna *ab initio* simulation program (VASP),²⁶ in the framework of DFT. The supercell with periodic boundary condition consists of six layers of Cu atoms in the (110) direction and a vacuum layer exceeding 23 Å. The water molecules are placed on one side of the slab in the periodicity of $c(2 \times 2)$. The calculated lattice constant of 3.6349 Å for face-centered-cubic Cu is used, which compares well to the experimental value of 3.6149 Å. For convenience, we use the experimental lattice constant for all other metal systems.

We use projector augmented plane waves method²⁷ and Perdew-Burke-Ernzerhof exchange-correlation functional²⁸ as implemented in VASP, which are reliable in describing the hydrogen bonds and bulk properties of water²⁹ as well as surface properties.³⁰ A plane wave cutoff of 400 eV and k -point mesh of $(2 \times 2 \times 1)$ in the Monkhorst-Pack sampling scheme³¹ are used. Gaussian smearing with a width of 0.2 eV is used. The free energy was extrapolated to zero Kelvin to yield total energies of the systems. This set of parameters assures a convergence of 0.01 eV/atom in total energy. Adsorption energy (E_a) is defined as the energy difference per water molecule between the adsorption system and that of separated substrate and water molecules in gas phase throughout this paper.

In the structural search, the bottom three layers of Cu substrate are fixed at their respective bulk positions, while all other atoms and water molecules are allowed to fully relax until forces on them are less than 0.05 eV/Å. In molecular dynamics (MD) simulations, the first three layers of Cu (110) surface atoms and water molecules were allowed to move according to the forces calculated from the converged electronic structure, employing Born-Oppenheimer approximation. A time step of 1 fs was utilized. The trajectories were collected through a 2.5 ps production run at 80 K using Nose thermostat³² after equilibrating the system for 1 ps. Fourier transform of the dipole-dipole correlation function along surface normal (z) recorded in the MD simulations yields vibration spectra for the systems. Reaction barriers are calculated using the nudged elastic band (NEB) method.³³ The NEB method yields the globally optimized path rather than the locally restricted one (as in constrained optimization techniques), and is, therefore, more reliable.

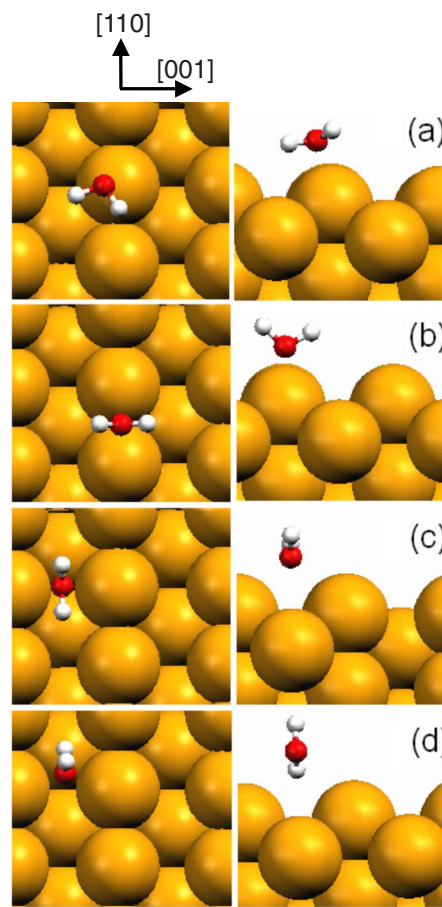


FIG. 1. (Color online) Adsorption configurations of a water molecule on Cu(110), shown in both top and side views: (a) top site, (b) bridge site along $[110]$, (c) bridge site along $[001]$, and (d) hollow sites. Red balls for oxygen, white for hydrogen, and orange for copper.

III. RESULTS AND DISCUSSION

A. Single water molecule on Cu(110)

1. Adsorption

To start, we investigate the interaction of a single water molecule with the Cu(110) surface, since in this case only water-Cu interaction is involved, without any contribution from intermolecular hydrogen bonding between water adsorbates. Four different possible sites have been considered, including the top site, two bridge sites (along $[110]$ and $[001]$ directions, respectively), and the hollow site, as shown in Fig. 1. Their respective averaged Cu-O and O-H bond lengths, HOH bond angles in water, and adsorption energies are summarized in Table I.

In Table I, the bond length of Cu-O on the top site [Fig. 1(a)] is 2.18 Å, smaller than that on the bridge sites (2.37 and 2.64 Å, respectively) and on the hollow site (3.13 Å). The largest binding energy is observed for water on the top site (0.375 eV), so a single water prefers to adsorb atop. Although the OH bond lengths are nearly the same (0.98 Å) for all the four sites, they are the longest for water on the top site. This comes from stronger Cu-O binding, resulting in

TABLE I. Calculated geometrical parameters and the adsorption energy (E_a) for single water molecule adsorption on different sites of the Cu(110) surface.

Adsorption sites	d_{CuO} (Å)	d_{OH} (Å)	\angle HOH (deg)	E_a (eV)
Top	2.18	0.981	105.0	0.375
Bridge [110]	2.37	0.978	108.5	0.221
Bridge [001]	2.64	0.977	106.7	0.142
Hollow	3.13	0.979	104.9	0.174

larger charge transfer from O to Cu, thus weakening the O-H bond in water. We note that water deviates from the exact top site by 0.5 Å, which is generally much larger than that on close-packed metal surfaces.³⁴ The HOH angles on the top and hollow sites are also very close (104.9°), while that on the two bridge sites are enlarged to 108° and 106° because of the Cu-H attraction. Finally, it is worth mentioning that the most favorable site for H₂O on Cu(110)—top site, with a flat-lying geometry—is the same as many closely packed metal surfaces, including Pt(111), Pd(111), Rh(111), and Ru(0001),³⁴ and various Cu surfaces, ranging from Cu(100), Cu(111), to Cu(211),²² albeit the quantitative geometrical parameters and energies vary from case to case. These results clarify earlier speculations of water adsorption on hollow¹⁴ or bridge sites.¹⁵

2. Diffusion

It is observed that water diffuses easily on metal surfaces, even at temperatures as low as 20 K.³⁵ On Cu(110) surface, we calculated that the diffusion barrier for a single water along [110] direction is 0.12 eV, and that along [001] is 0.23 eV. Both are very small, and can be compared with the experimental measured value of 0.13 eV for water/Pd(111).³⁶ The diffusion paths run across the bridge sites so that bridge-site adsorption serves as the transition states. The calculated barriers are consistent with that estimated from adsorption energy difference on different sites. Moreover, water diffusion along [110] is much easier than along [001] due to its half-size smaller activation energy. This anisotropic behavior arises from the asymmetric potential surfaces, which in turn originates from the asymmetric geometry of the (110) surface—the Cu-Cu distance along [110] is 2.57 Å, while that along [001] is 3.63 Å. Water diffusion might also be sensitive to the orientation of water molecules.³⁷ The small barriers of a single water indicate that water diffuses readily along both [110] and [001] directions, even at low temperatures >50 K. This will favor water cluster formation.

3. Dissociation

Based on the above structural analysis, we study the dissociation process of a single water molecule on Cu(110) surface. Figure 2 presents the relevant energy barrier and minimum energy path of a single H₂O dissociation. When a single water molecule moves from the initial state [Fig. 2(a)] to the intermediate precursor state [Fig. 2(b)], the energy increases slightly, by 0.034 eV only. Moreover, the adsorb-

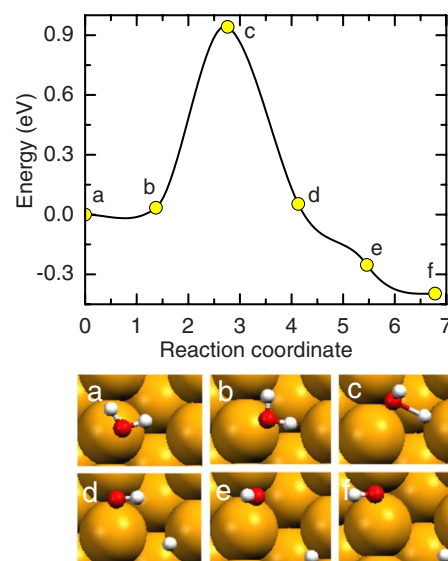


FIG. 2. (Color online) Minimum energy pathway for a water molecule dissociation on Cu(110) surface. Typical configurations sampled along the pathway [labeled as (a)–(f)] are depicted in bottom panels.

ing site of H₂O is still on the top site with a larger lateral displacement toward the bridge site (1.03 Å), but a small variation in O-H bonds (elongated by 0.01 Å).

However, in the transition state [Fig. 2(c)], not only one of the O-H bond length reaches 1.55 Å, the O atom also relocates to a place very close to the [110] bridge site. The energy of the system increases sharply to 0.94 eV higher than the initial configuration, indicating a barrier of 0.94 eV for a single water molecule dissociation. Compared with desorption or adsorption energy of 0.38 eV, the water molecule has a very low rate to dissociate on Cu(110), while desorption and diffusion are much more favorable.

After dissociation, the O-H bond is broken and the energy of the system decreases gradually. The bound OH group relocates to the bridge site with a binding energy of 3.69 eV, and H binds in the groove with an energy of 2.37 eV, forming three Cu-H bonds [Fig. 2(f)]. The overall binding energy in the final configuration is 0.77 eV relative to gaseous H₂O, 0.4 eV more stabilized than the initial intact adsorption. Considering the bound energy of a OH bond in H₂O is 5.21 eV (calculated), this number is reasonable because 3.69+2.37–5.21=0.85 eV, close to 0.77 eV. Therefore, water dissociation on Cu(110) is exothermic. Previous assignment of water binding on bridge sites of Cu(110) (Ref. 15) could result from a small amount of OH groups after H₂O dissociation residing on more favorable [110] bridge sites.

B. Water monolayers

1. Possible structural models

Because a water molecule is very unlikely to dissociate, while very easy to diffuse in both directions on Cu(110), it would form clusters favored by the formation of two to three H bonds per H₂O between water molecules. One particular case is what happens when the surface is fully covered by

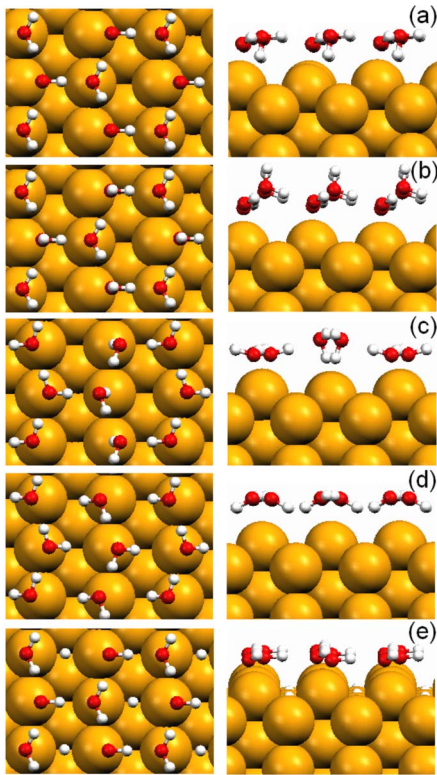


FIG. 3. (Color online) Atomic structure of the [(a)–(d)] intact and (e) half-dissociated water overlayers at 1 ML on Cu(110): (a) H-down bilayer, (b) H-up bilayer, (c) chainlike bilayer, (d) square-like layer, and (e) half-dissociated layer. Both top and side views are shown.

water, i.e., at the Cu:H₂O ratio of 1:1 (i.e., 1 ML). It is observed that water wets the Cu(110) surface.^{14–18} So at the coverage of 1 ML, water will form two-dimensional extended adlayers. There are many possible structures for this coverage at the atomic level. Of particular interests are those that are termed as an “ice bilayer,” which has a puckered hexagonal network with one OH bond for every two waters, pointing to [H-down, Fig. 3(a)] or away from the surface [H-up, Fig. 3(b)]. Our calculation shows that the adsorption energy of H₂O in the H-down bilayer is 0.554 eV/H₂O, which is much higher than that in the H-up bilayer with 0.514 eV/H₂O. It is obvious that the H-down bilayer is more stable than the H-up bilayer. Previously, the H-down bilayer has been identified for water on Pt(111) from x-ray absorption experiments.³⁸

At the same time, we also calculate other possible monolayer structures, as shown in Figs. 3(c) and 3(d). Figure 3(c) has the same geometry as H-down [Fig. 3(a)] for oxygen atoms, but protons are placed quite differently: it is referred to as one of the “proton-disordered” structures. Particularly,

in Fig. 3(c), water forms a linear chain along [110], with one of its two OH groups pointing to its neighbors along the [110] direction and the other points to [00–1] and [001] alternately. This structure has been calculated to be the most stable structure among intact water overlayers on Ru(0001) (Ref. 39) [0.13 eV more stable than Fig. 3(a)], but on Cu(110), it is almost energetically degenerate with structure Fig. 3(a)—the tiny difference of 0.006 eV is within the computation accuracy. We further find that different proton order patterns result in a typical energy difference less than 0.018 eV, therefore proton disorder does not make a big difference for water on Cu(110). Figure 3(d) is the optimized structure from a configuration where each Cu atom has a water adsorbed on the top site [$p(1 \times 1)$]. The adsorption energy is 0.442 eV/H₂O, much lower than the cases of Figs. 3(a)–3(c). We have also tried water structures which have hexagonal patterns, with one-third OO bonds parallel to [110] [so it can be considered as structure Fig. 3(a) rotated by 90° with the substrate fixed]. It is not stable and will transform into structure Fig. 3(a) after optimization.

However, once the non-hydrogen-bonded OH breaks, it will form the half-dissociated overlayer as Feibelman proposed for the Ru(0001) case [Fig. 3(e)]. The OH remains on the top sites, and the dissociated H atom resides on the four-fold position in the groove. Interestingly, the adsorption energy of the dissociated water layer with 0.632 eV/H₂O is significantly higher than that of both water bilayer (0.554 eV/H₂O for H-down and 0.514 eV/H₂O for H-up), similar to the situation of water on Ru(0001).¹¹ This is consistent with experimental observations that hydroxyl groups anchor water molecules and enhance the stability of OH + H₂O overlayers on Cu(110).^{7,8} The vertical OO distance in the half-dissociated water layer is 0.10 Å, much smaller than that of H-down (0.38 Å) and H-up (0.76 Å) bilayers. In addition, the top site adsorption is preferred for the mixed OH+H₂O layer, which is at least 0.07 eV/H₂O more favorable than the bridge site. This rules out most of the structural models assumed previously.^{16,40}

2. Intact or dissociated?

To determine the real structure observed in low-temperature experiments, we calculate the work function change $\Delta\Phi$ upon adsorption relative to the clean surface, as shown in Table II. A decrease of work function for intact adsorption (–0.8 eV for H-down, and –3.6 eV for H-up bilayers) and an increase for the half-dissociated overlayer (1.0 eV) are observed. It is interesting that a decrease of 0.3 eV in work function was calculated for half-dissociated layer on Ru(0001),¹¹ contrasting with the increases of 1.0 eV on Cu(110). Comparing with the experimental value of –(0.9–1.0) eV,^{14–16} this strongly suggests intact adsorption over dissociation. Furthermore, $\Delta\Phi = -0.8$ eV for H-down

TABLE II. Work function change of various water overlayers on Cu(110) relative to clean surface.

	H-down	H-up	Mixed (1:1)	Dissociated	Experiment ^a
$\Delta\Phi$ (eV)	–0.8	–3.6	–2.1	+1.0	–(0.92–1.0)

^aReferences 14–16.

bilayer is the closest to experimental value, indicating the majority of H-down bilayers in experiment. Work function change for the chain structure in Fig. 3(c) is -0.9 eV, also very close to the H-down bilayer. This is, once again, contradicting the case on Ru(0001), where the chain structure has a very large work function change ($\Delta\Phi = -1.15$ eV) compared with that for the H-down bilayer ($\Delta\Phi = -0.4$ eV).³⁹ Therefore, contrary to the suggestion that the chain structure serves as a more plausible model for water/Ru(0001), this structure has almost the same characteristics as the H-down bilayer on Cu(110), and can be considered as the derivation from the more general H-down bilayer model.

Because $\Delta\Phi$ is a surface average quantity, we infer that a mixture of H-up:H-down=1:13-1:23 could reproduce better the experimental measured values. This idea is verified by $\Delta\Phi = -2.1$ eV for a mixed bilayer of H-up:H-down=1:1, very close to the average value of -2.2 eV. Furthermore, we find that the adsorption energy for this mixed bilayer is 0.553 eV. The difference of 1 meV relative to the pure H-down bilayer is within the calculation accuracy, indicating it is at least as stable as the pure H-down bilayer. In addition, the H-up/H-down conversion is highly accessible because of the small energy barrier in between [76 meV on Pt(111) (Ref. 41) and 55 meV on Ru(0001) (Ref. 43)]. All these point to the (H-up+H-down) mixture structure model for intact water adlayers on Cu(110). Recently, x-ray absorption and XPS studies have suggested a H-down:H-up ratio of 2:1 in the (7×8) phase (where the H-down component contributes a major percentage of 66%), consistent with our assignment.²⁰ More critically, the appearance of the vibrational peak at 457 meV in the reflection adsorption infrared spectroscopy (RAIRS), which arises from the free OH stretch mode,²⁰ clearly points to the existence of the H-up component. This feature cannot be reproduced by either the pure H-down [Fig. 3(a)] or the pure chain structure [Fig. 3(c)] though its work function change is closer to experiment.

To understand the bonding nature between water and Cu(110), we plot the charge density difference in Fig. 4. It is clearly shown that water-Cu interaction involves mainly O lone pairs and Cu p_z states. OH group interacts with Cu more strongly, resulting in accumulation of 1π states and depletion of Cu d_{z^2} states. This is more prominent in the one-dimensional charge density plot in Fig. 4(c). Integrating this curve along surface normal z suggests $0.17e$ per cell transferred from water to Cu(110) for the H-down bilayer, and $0.14e$ from Cu to adsorbate for dissociated layer. This perfectly explains the opposite sign of $\Delta\Phi$ in Table II.

Furthermore, the calculated vibration spectrum for the H-down bilayer agrees with experiment excellently.²⁵ Both the peak shape and positions of libration modes at 94 meV, HOH scissor modes at 195 meV, and OH stretch modes at 406 and 418 meV agree well with experimental vibrations at 93, 200, and 411 meV at 110 K.¹⁶ It also qualitatively agrees with the new RAIRS measurement for the (7×8) structure, where dominant peaks are 103, 201, and 420–457 meV, and no features appear in the range from 103 to 201 meV.²⁰ The free OH stretch mode at 457 meV observed in RAIRS will be clearly present if the H-up bilayer component is included,

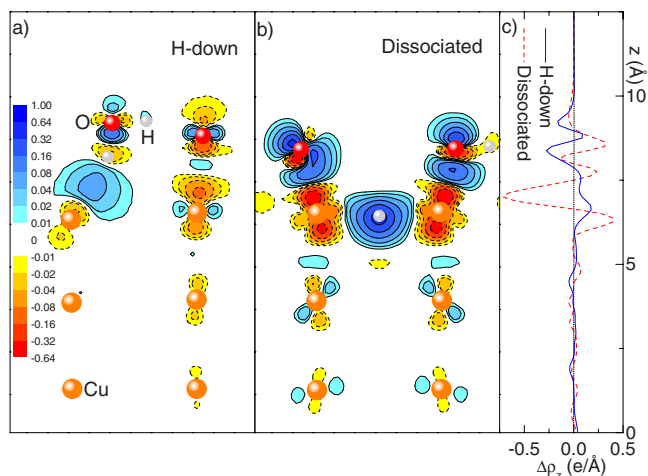


FIG. 4. (Color online) Contour plot of the charge density difference (in unit of $e/\text{\AA}^3$) between the total system and that of separate substrate and adsorbate layer upon (a) intact (H-down) and (b) half-dissociated water adsorption. Horizontal axis is the [001] direction that goes through O-O, and vertical axis is surface normal z . (c) Planar averaged charge difference along z for the two structures.

as this is the case on Pt(111) (Ref. 42) and Ru(0001).⁴³ On the contrary, the vibration spectrum for the half-dissociated overlayer is very different from experiment, e.g., OH stretch at 433 meV and libration at 122 and 111 meV. The Cu-H vibration at 154 meV is also missing in experiments. Based on this comparison, we can safely rule out the half-dissociated component in the experiments.

3. Why intact: Water dissociation pathway

It seems safe to conclude that the $c(2 \times 2)$ water adlayer on Cu(110) in low-temperature experiments is intact as opposed to the half-dissociated structure model. The question arises: Why does water not dissociate under these circumstances even though the half-dissociated structure is energetically more favorable?

To answer it, we have studied the dissociation process of 1 ML water layer on Cu(110) surface. The relevant energy barrier and minimum energy path for water dissociation in 1 ML water adlayer are shown in Fig. 5. When the water layer changes into the precursor state (not shown) from its initial H-down configuration [Fig. 5(a)], the energy changes slightly by 0.025 eV only, while a pair of water molecules sitting along [110] come closer by 0.1 Å. However, in the transition state [Fig. 5(b)], the OH bonds of the two water molecules are broken to release two H atoms and two OH groups. Simultaneously, the newly formed OH group located upper in Fig. 5(b) (molecule 1) captures the H atom donated by the lower water (molecule 2) and forms a new molecule. Consequently, the net result is that molecule 2 dissociates into an OH group, still on top site, and the H atom originally coming from molecule 1 remains isolated, bonding at the [110] bridge site. This is a *late* transition state because it largely resembles the final state where water is fully dissociated. The energy of the system in the transition state increases sharply to 0.57 eV, revealing a barrier of 0.57 eV for

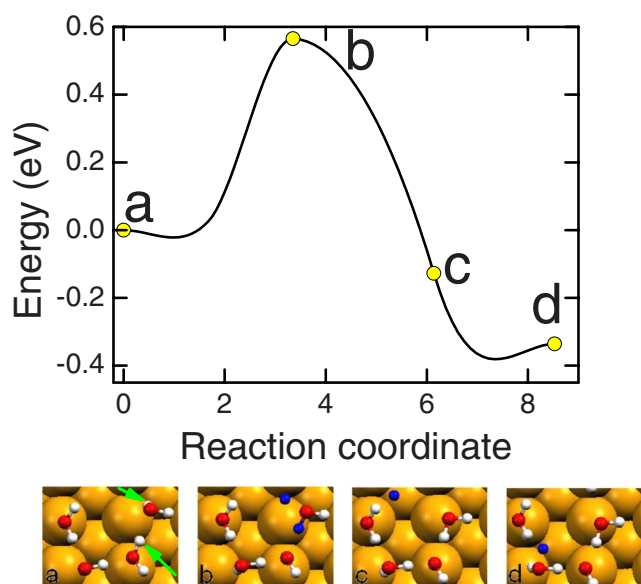


FIG. 5. (Color online) Dissociation pathway for a water molecule in the 1 ML H-down bilayer on Cu(110). Only important structural snapshots along the pathway are shown. Arrows in snapshot (a) indicate which H is dissociated.

water dissociation in the 1 ML water adlayer. This barrier agrees well with the measured value of 0.53–0.56 eV from the temperature-programmed XPS experiment,²¹ which suggests that the finite size of the supercell used in our calculation may not have a significant influence on the dissociation process. With zero-point energy correction, the theoretical value is reduced by ~ 0.1 eV,⁴⁴ but it is argued that the plane-wave methods adopted here usually underestimate reaction barriers.⁴⁵ After water dissociation in the monolayer, the dissociated OH group still sits on the top site and the isolated H atom continues to move into the groove. The energy gradually decreases to -0.336 eV. Because only one-fourth water molecules are dissociated in Fig. 5(d), the final H configuration is slightly different from the half-dissociated overlayer in Fig. 3(e).

In the above mechanism for water dissociation in the monolayer, multiple proton transfer processes are involved: proton transfer from molecule 1 to beneath Cu atoms, and from molecule 2 to molecule 1 along the hydrogen bond formed between them. The two processes almost occur simultaneously; several trials launched to locate which process is earlier along the dissociation pathway failed. We also found that the double proton transfer mechanism is probably necessary to lower the dissociation barrier to 0.57 eV. The dissociation pathway that directly splits the OH bond by the surface Cu atoms without H transfer in neighboring molecules (from molecule 2 to 1) has a barrier of 1.10 eV. Another pathway where an intermediate H_3O^+ group is formed before breaking the OH bond and transferring H to the surface has a very large barrier of 2.70 eV, indicating that such a process is highly unfavorable and proton transfer and OH breaking has to be simultaneous. A third dissociation pathway which does not have the H on the Cu-Cu bridge sites as transition state but involves H at the three-coordinated site as

in Fig. 2(f) has also a larger barrier of 1.09 eV. Prompt proton transfer was observed in MD simulations of a wetting water layer on Pt(111) at 130 K.⁴⁶ The lack of an assisting proton transfer process may explain why Tang and Chen failed to identify a low dissociation barrier in water monolayers.²³ These pathways with a high energy barrier (>1.1 eV) do not agree with the measured values of 0.53–0.56 eV in most recent experiments.²¹

After dissociation, the overall binding energy in the final configuration is 0.63 eV, about 0.08 eV more stabilized than the initial molecular adsorption. Moreover, the Cu-O bond length is 1.93 Å, far less than that in the intact bilayer (2.27 Å). The small bond length also emphasizes the largest binding energy (0.63 eV). In addition, the significant change of the vertical OO distance from 0.38 Å in the intact adsorption configuration to 0.03 Å in the dissociated state also suggests that after dissociation, the water layer will gradually adopt a flat geometry.

Comparing with the barrier of 0.94 eV in a single water dissociation, the barrier of 0.57 eV in 1 ML overlayer points out that additional water lowers the activation energy. One may ask whether this is a consequence of direct water interaction with reactant (H_2O) and products ($\text{OH}+\text{H}$), or via indirect interactions mediated by the substrate. Our answer is that both factors play an important role, as exemplified by the double-proton transfer mechanism. The first factor, direct interactions between reactants (H_2O) and products ($\text{OH}+\text{H}$), namely, hydrogen bonds, lowers overall energy and dissociation barriers significantly. Whenever a water molecule is hydrogen bonded, whether as a proton donor or an acceptor, its own OH bond is weakened, facilitating dissociation. This can be verified by the fact that the dissociation barrier in a free water molecule (5.21 eV, without H bonds) is lowered to 1 eV in bulk water.⁴⁷

However, on surfaces, water dissociation usually goes through non-hydrogen-bonded OH bonds, which points to the importance of water-substrate interaction. Specifically, water dissociation proceeds through H-Cu interactions, which finally break the O-H bond and make new H-Cu bonds. Whether reaction products are stable and how large the reaction barrier is depends much on the bond strength of the H-Cu (also Cu-OH) bond in the final state and the intermediate transition state. Addition of water molecules help to establish hydrogen-bond networks restricted to the substrate periodicity, in which some water are held in a “precursor” state (H-down species) where H-Cu interactions are stronger. Water donates electrons to surface Cu, which also strengthens the H-Cu bond indirectly. H-bond strengths are also mediated by the substrate, which will affect the OH bond strength. In other words, the interplay of H bonds and substrate restriction, resulting in water molecules in geometries and bonding environment that favor dissociation, is the main cause of the lowering of dissociation barriers, though we cannot tell which effect dominates.

Our results are quite similar to that on Ru(0001). Feibelman correctly predicted that the half-dissociated water adlayer on Ru(0001) is energetically favorable, but ignored kinetic constraints that block water dissociation. We present a complete comparison between the two interesting systems in the following:

(i) Both Feibelman and us have found that the half-dissociated overlayer is more stable than intact bilayers. Adsorption energies on Ru(0001) are 0.66 eV/H₂O for dissociated adlayers and 0.50 eV/H₂O for intact bilayers;¹¹ on Cu(110), they are 0.63 eV/H₂O for dissociated and 0.55 eV/H₂O for intact overlayers.

(ii) On Ru(0001), calculated vibration frequencies for the dissociated layer by Feibelman⁴⁸ do not agree with experimental high-resolution electron-energy-loss spectroscopy spectra.⁴⁹ On Cu(110), calculated vibration spectra for the dissociated layer do not agree with experiments either, while the calculated spectra for intact bilayer agree with experiments very well.

(iii) Feibelman calculated a work function change of 0.3 eV for the dissociated layer on Ru(0001), at variance with the measured one: 1.3 eV. However, he discarded this comparison, arguing that other water species may also contribute to the measured work function.¹¹ Our calculations show a work function change of +1.0 eV for dissociated layer on Cu(110), contradicting experiment: -0.92 eV. Instead, intact H-down bilayers have a very close work function change of -0.8 eV.

(iv) Unfortunately, Feibelman did not calculate the dissociation barrier, which may block the dissociation kinetically before desorption, though the dissociated layer is energetically favorable. Later studies by Michaelides *et al.*⁵⁰ and us⁴³ indeed, suggested this behavior. The barrier for water dissociation on Ru(0001), 0.50–0.62 eV, hinders water dissociation in the intact wetting D₂O layer as confirmed in a recent experimental study.¹³ On Cu(110), our calculated barrier of 0.57 eV not only agrees with the experimental activation energy, but also predicts the same behavior of water: water adsorbs molecularly, and the dissociation is constrained by a larger barrier than desorption (barrier: 0.55 eV).

Summarizing the above, we have found a very similar behavior of water on Ru(0001) and on Cu(110), despite some significant differences such as the presence of isotopic effects on Ru(0001).⁵¹ However, by taking a complete consideration over all factors and making better comparison with experiments, we have reached a different conclusion from Feibelman's. Feibelman has given *correct* results, but may be *incomplete*. Only considering energetics and geometries would very likely lead to overlooking many other factors that dominate the observed surface phenomena, such as kinetics. Indeed, after five years of intensive study, both experimentally and theoretically, on water/Ru following Feibelman's suggestion, the general consensus is that the intact bilayer and the half-dissociated adlayer could both exist before and after beam damage, respectively.^{12,13,43,49} We expect that water dissociation on Cu(110) would be even more sensitive.²¹

4. Hydrogen kinetics

After water dissociation in 1 ML, H is held in the [110] channel and at the center of water hexagons, forming four Cu-H bonds with a bond length of 1.79 Å. It is very interesting that the dissociated H atoms can easily diffuse away along the [110] channel. The diffusion pathway is shown in Fig. 6. The diffusion barrier is calculated to be as low as 0.23 eV. Zero-point energy correction will further lower this

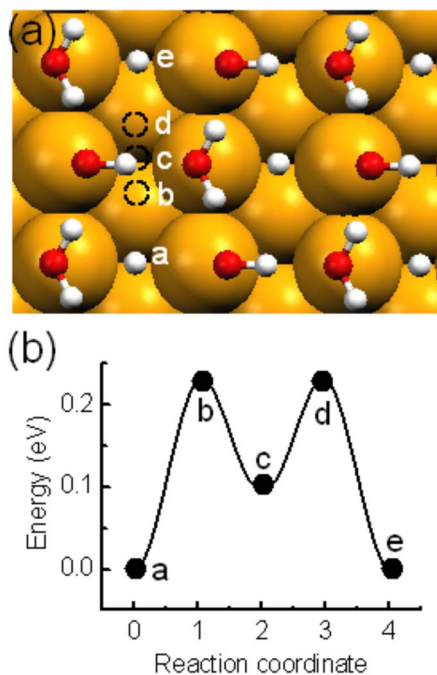


FIG. 6. (Color online) (a) Diffusion pathway and (b) the corresponding energy change for a single H atom in the half-dissociated water layer on Cu(110).

barrier significantly. The calculated H vibration energy of 154 meV at the fourfold site would render a zero-point energy of 0.077 meV, reducing the barrier to ~ 0.15 eV. In addition, quantum tunneling of proton is highly possible because of its small mass. All these will facilitate H diffusion at a low temperature, ~ 90 K or even lower. We emphasize that the presence of water overlayers do not obviously influence the H diffusion process. The diffusion of a H atom in [110] channels on a clean Cu(110) has a barrier of 0.21 eV, close to 0.23 eV here, though the most stable position for a free H is the three-coordinated position as in Fig. 2(f). This is in contrast with the behavior of water dissociation on Ru(0001), where H is held at the center of the water hexagon, but does not form separate H patches on Ru(0001), evidenced by the D titration experiment.⁵² Half-dissociation of water on Cu(110) then provides a promising route for H₂ and O₂ separation in the thermal splitting of water.

C. Water on other noble metal (110) surfaces

In order to study further the interaction of water molecules with noble metal (110) surfaces and to find the general trends, we have chosen several other representative metal (110) surfaces, including Ag, Au, Pd, and Pt. Due to the lower surface energy, Pt(110) and Au(110) prefer to form the missing row (1×2) reconstructed surfaces, as found in experiment (see Refs. 53 and 54). For comparison, we have included both the reconstructed and unreconstructed (110) surfaces for Pt and Au.

First, as on Cu(110), we study a single water molecule adsorption on these metal (110) surfaces. The adsorption energy of a single H₂O on the top site is calculated to be in the

TABLE III. Parameters of an intact water molecule or dissociated (OH+H) group binding on different metal (110) surfaces. d_{MO} represents the metal–O bond length.

Metal	Intact		Dissociation	
	E_a (eV)	d_{MO} (Å)	E_a (eV)	d_{MO} (Å)
Cu	0.375	2.20	0.772	1.95
Ag	0.236	2.54	−0.267	2.20
Au	0.213	2.59	−0.377	2.18
Au(1×2)	0.168	2.73	−1.583	2.24
Pd	0.414	2.30	0.243	2.11
Pt	0.597	2.23	0.772	2.12
Pt(1×2)	0.423	2.28	0.231	2.12

order of Pt>Pt(1×2)>Pd>Cu>Ag>Au>Au(1×2), ranging from 0.60 to 0.17 eV (see Table III). Overall, the adsorption energies are close to each other and the curve of the relative energy (i.e., $-E_a$) for these systems is relatively flat [Fig. 7(a)]. In particular, for Cu, Ag, and Au, which belong to the same element group IB, the adsorption energy of H₂O/Cu(110) is 0.375 eV, much higher than that of Ag (0.236 eV), Au (0.213 eV), and Au(1×2) (0.168 eV). This indicates an order of Cu>Ag>Au in chemical reactivity for these surfaces, in accord with the general belief. In addition, the Cu–O bond length of 2.20 Å is clearly shorter than the Ag–O bond (2.54 Å) and Au–O bond [2.59 Å for Au and 2.73 Å for Au(1×2)], consistent with the trend in adsorption energy. Comparing the adsorption energy of H₂O/Pd and H₂O/Pt, the latter has an energy of 0.597 eV, much

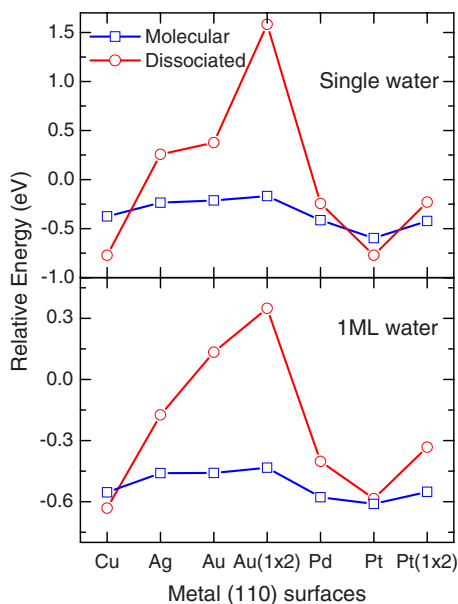


FIG. 7. (Color online) Relative energy ($-E_a$) for (a) an intact and dissociated (i.e., OH+H group) water molecule and (b) a monolayer of molecular (H-down) and half-dissociated water overlayer on different noble metal (110) surfaces. Au(1×2) and Pt(1×2) surfaces are missing-row reconstructed surfaces.

higher than the former by 0.414 eV. However, this difference diminishes when the (1×2) missing-row reconstruction of Pt(110) is taken into consideration, where the energy goes down to 0.423 eV. Moreover, the metal–O bond length in the two systems is very close, 2.30 and 2.28 Å, respectively.

Once one OH bond is broken, H₂O is dissociated. The system of the (OH+H) group on the above metal (110) surfaces is subject to structural optimization, which results in adsorption geometries very similar to that on Cu(110) [Fig. 2(f)]. The trend in the adsorption energy immediately becomes Pt>Cu>Pd>Pt(1×2)>Ag>Au>Au(1×2). It is shown that the adsorption energy for both Cu and Pt (110) surfaces increases sharply to 0.772 eV, but the energy decreases for the other metal surfaces compared with intact adsorption. The increased adsorption energy indicates the stabilization of water molecules after dissociation. Very interestingly, the binding energy of (OH+H) on Ag and Au is negative (repulsive interaction), while on Cu, Pt, and Pd it is positive (attractive interaction), indicating corrosion by water is prevented on the former two surfaces. It is worthy to point out that, although water dissociation is favored on the Pt(110) unreconstructed surface, the adsorption energy of (OH+H) on the stable phase of the Pt(110)(1×2) surface (0.231 eV) is smaller than that of intact adsorption (0.423 eV). Therefore, based on the comparison of the adsorption energies between intact and dissociative adsorption, we found that a single water dissociation is favored only for H₂O/Cu(110). For the rest of the systems, an intact water molecule is more stable instead.

More useful information comes from the full water overlayer adsorption on these noble metal (110) surfaces. We have calculated the adsorption energies of both the molecular and the half-dissociated water overlayer at the coverage of 1 ML. The H-down bilayer structure is taken as the representative model for intact overlayer adsorption because of its high stability and simplicity. Figure 7(b) shows the corresponding adsorption energy of H₂O overlayers on metal (110) surfaces. The general trend in energetics is almost the same as the single water adsorption, except for a minor order switch for Pd and Pt(1×2), that is, Pd (0.578 eV)>Pt(1×2) (0.551 eV). The corresponding energies, metal–O bond lengths, and the OO distance in surface normal direction (film thickness) are summarized in Table IV. The very small vertical OO distances after dissociation show that the half-dissociated water layer is flat, with H₂O and OH layers located in the same plane.

Only the adsorption energy of H₂O/Cu(110) goes up after half-dissociation in 1 ML adlayer takes place, and all other surfaces have a smaller binding energy than intact bilayers. The Au and Au(1×2) surfaces have negative adsorption energies for the half-dissociated overlayer in contrast to other surfaces, indicating dissociated water adlayers do not bind on Au surfaces. This partly explains the nobility of gold. For all cases (Pt vs Au, molecule vs monolayer, and intact vs dissociative), the (1×2) missing-row reconstruction lowers the water adsorption energy, and thus makes the clean surface less reactive or more stable after reconstruction. This is more prominent if we compare Pd(110) and Pt(110). Overall, both surfaces are very close in reactivity (Fig. 7). The unrecon-

TABLE IV. Bond lengths of the metal–O bonds (d_{MO}) and the vertical O–O distances (z_{OO}) for the intact and half-dissociated H_2O monolayer on noble metals (110) surfaces.

Metals	Intact			Dissociation		
	E_a (eV)	d_{MO} (Å)	z_{OO} (Å)	E_a (eV)	d_{MO} (Å)	z_{OO} (Å)
Cu	0.554	2.27	0.38	0.632	1.93	0.03
Ag	0.460	2.68	0.17	0.174	2.18	0.06
Au	0.459	2.72	0.22	−0.134	2.17	0.08
Au(1×2)	0.430	2.82	0.19	−0.349	2.08	0.01
Pd	0.578	2.37	0.32	0.402	2.07	0.12
Pt	0.611	2.29	0.49	0.585	2.08	0.05
Pt(1×2)	0.551	2.22	0.45	0.332	1.99	0.02

structed Pt(110) surfaces seem to be more reactive than Pd(110), evidenced by the larger adsorption energy of the intact and dissociated water molecules and overlayers. However, as Pt(1×2) is the stable phase at room temperature, the reactivity is largely reduced to the same level as or even less than Pd(110) after surface reconstruction of Pt(110). For instance, the adsorption energy of the half-dissociated water layer on Pd, Pt, and Pt(1×2) surfaces is 0.402, 0.585, and 0.332 eV/ H_2O , respectively, following this trend.

The larger adsorption energy of the half-dissociated layer than the molecular bilayer on Cu(110) indicates that the dissociated H_2O overlayer is more stable than intact adsorption, in contrast with all other surfaces considered here. Therefore, Cu(110) is certainly more reactive than inert Ag and Au (110) surfaces, and a little bit more reactive than Pd and Pt (1×2) surfaces, too. Considering that most of the metal surfaces such as Na and Fe are reactive to water adsorption, the behavior of water on Cu(110), especially water overlayers, has intermediate binding energy for both intact and dissociative adsorption, suggesting Cu(110) as the borderline for water dissociation. Indeed, the energy difference for intact and half-dissociated water overlayers is only 0.08 eV/ H_2O , the smallest among surfaces studied except Pt(110). Although the energy difference on Pt(110) is even smaller, the surface reconstructs into the less reactive (1×2) missing-row structure in experiments and, therefore, does not represent a realistic case. What follows is the Pd(110) surface, which has also a small energy separation between intact and dissociative water-layer adsorption, 0.18 eV. Interestingly, this seems to be consistent with earlier theoretical⁵⁵ and experimental studies⁵⁶ which identified Pd(111) as a borderline for dissociative water bilayer or cluster adsorption. For comparison, the energy difference for another borderline, Ru(0001), is 0.16 eV/ H_2O .¹¹ Here, the barrier between intact and dissociated states on Cu(110) is only 0.57 eV, which could be overcome by electron or photon illumination or thermal activation. In the experimentally observed (7×8) phase,²⁰ we expect this barrier be modified only slightly because the local bonding environment for the water molecule would be rather similar. The low dissociation barrier explains the experimental observation of the mixed H_2O and OH structures on Cu(110) at near-ambient conditions.⁷

IV. CONCLUSIONS

In conclusion, we have studied adsorption, diffusion, and dissociation of a single water molecule and 1 ML water overlayer on Cu(110) and other noble metal (110) surfaces. We provide conclusive evidences for the existence of intact bilayer on Cu(110) consisting of mainly H-down bilayers in low-temperature experiments, based on the following facts:

(1) A single water adsorbs intact on top site; it diffuses easily, while dissociation is blocked.

(2) The H-down bilayer has the largest adsorption energy (0.55 eV) among intact overlayers, though the half-dissociated layer is 0.08 eV more stable.

(3) Work function decreases for intact water adsorption, but increases for the half-dissociated water layer; experiments found a negative change of $-(0.92-1.0)$ eV, close to H-down bilayers.

(4) The calculated vibration spectrum for the H-down bilayer shows vibration modes at 94, 195, 406, and 418 meV, agreeing with experimental observations; while it shows many unobserved peaks around 100–150 meV for the half-dissociated layer. The peak at 457 meV in experiment points to the existence of the H-up component.

(5) Both theory and experiment found a barrier about 0.57 eV for water dissociation in overlayers, slightly higher than the desorption barrier.

Comparison with water adsorption on other noble metal surfaces identifies Cu(110) as the borderline for intact and dissociative water adsorption, with the smallest energy separation between the two structures (0.08 eV/ H_2O). Our results show that considering DFT energy alone is dangerous in determining structures observed in experiment. Much attention has to be paid to comparisons such as work function change, kinetic barriers, and spectroscopic characters.

ACKNOWLEDGMENTS

The authors acknowledge the insightful discussion with Efthimios Kaxiras. The authors thank Theanne Schiros for her careful reading of the manuscript. This work is partially supported by the U.S. Department of Energy and the Harvard University Center for the Environment.

- ¹G. Ertl, *J. Vac. Sci. Technol. A* **1**, 1247 (1983).
- ²N. A. Koryabkina, A. A. Phatak, W. F. Ruettinger, R. J. Farrauto, and F. H. Ribeiro, *J. Catal.* **217**, 233 (2003).
- ³C. Callaghan, I. Fishtik, R. Datta, M. Carpenter, M. Chmielewski, and A. Lugo, *Surf. Sci.* **541**, 21 (2003).
- ⁴P. A. Thiel and T. E. Madey, *Surf. Sci. Rep.* **7**, 211 (1987).
- ⁵M. A. Henderson, *Surf. Sci. Rep.* **46**, 1 (2002).
- ⁶J. Stahler, M. Mehlhorn, U. Bovensiepen, M. Meyer, D. O. Kusmierek, K. Morgenstern, and M. Wolf, *Phys. Rev. Lett.* **98**, 206105 (2007).
- ⁷S. Yamamoto, K. Andersson, H. Bluhm, G. Ketteler, D. E. Starr, T. Schiros, H. Ogasawara, L. G. M. Pettersson, M. Salmeron, and A. Nilsson, *J. Phys. Chem. C* **111**, 7848 (2007).
- ⁸K. Andersson, G. Ketteler, H. Bluhm, S. Yamamoto, H. Ogasawara, L. G. M. Pettersson, M. Salmeron, and A. Nilsson, *J. Phys. Chem. C* **111**, 14493 (2007).
- ⁹G. Held and D. Menzel, *Surf. Sci.* **316**, 92 (1994).
- ¹⁰J. Weissenrieder, A. Mikkelsen, J. N. Andersen, P. J. Feibelman, and G. Held, *Phys. Rev. Lett.* **93**, 196102 (2004).
- ¹¹P. J. Feibelman, *Science* **295**, 99 (2002).
- ¹²K. Andersson, A. Nikitin, L. G. M. Pettersson, A. Nilsson, and H. Ogasawara, *Phys. Rev. Lett.* **93**, 196101 (2004).
- ¹³N. S. Faradzhev, K. L. Kostov, P. Feulner, T. E. Madey, and D. Menzel, *Chem. Phys. Lett.* **415**, 165 (2005).
- ¹⁴A. Spitzer and H. Lüth, *Surf. Sci.* **376**, 120 (1982).
- ¹⁵C. Mariani and K. Horn, *Surf. Sci.* **126**, 279 (1983).
- ¹⁶D. Lackey, J. Schott, B. Straehler, and J. K. Sass, *J. Chem. Phys.* **91**, 1365 (1989).
- ¹⁷Ch. Ammon, A. Bayer, H.-P. Steinrück, and G. Held, *Chem. Phys. Lett.* **163**, 377 (2003).
- ¹⁸T. Yamada, S. Tamamori, H. Okuyama, and T. Aruga, *Phys. Rev. Lett.* **96**, 036105 (2006).
- ¹⁹A. Michaelides and K. Morgenstern, *Nat. Mater.* **6**, 597 (2007).
- ²⁰T. Schiros, S. Haq, H. Ogasawara, O. Takahashi, H. Ostrom, K. Andersson, L. G. M. Pettersson, A. Hodgson, and A. Nilsson, *Chem. Phys. Lett.* **429**, 415 (2006).
- ²¹K. Andersson, A. Gomez, C. Glover, D. Nordlund, H. Ostrom, T. Schiros, O. Takahashi, H. Ogasawara, L. G. M. Pettersson, and A. Nilsson, *Surf. Sci.* **585**, L183 (2005).
- ²²Q. L. Tang and Z. X. Chen, *Surf. Sci.* **601**, 954 (2007).
- ²³Q. L. Tang and Z. X. Chen, *J. Chem. Phys.* **127**, 104707 (2007).
- ²⁴G. C. Wang, S. X. Tao, and X. H. Bu, *J. Catal.* **244**, 10 (2006).
- ²⁵J. Ren and S. Meng, *J. Am. Chem. Soc.* **128**, 9282 (2006).
- ²⁶G. Kresse and J. Furthmüller, *Phys. Rev. B* **54**, 11169 (1996).
- ²⁷P. E. Blöchl, *Phys. Rev. B* **50**, 17953 (1994).
- ²⁸J. P. Perdew, K. Burke, and M. Ernzerhof, *Phys. Rev. Lett.* **77**, 3865 (1996).
- ²⁹D. R. Hamann, *Phys. Rev. B* **55**, R10157 (1997).
- ³⁰S. Kurth, J. P. Perdew, and P. Blaha, *Int. J. Quantum Chem.* **75**, 889 (1999).
- ³¹H. J. Monkhorst and J. D. Pack, *Phys. Rev. B* **13**, 5188 (1976).
- ³²S. Nose, *J. Chem. Phys.* **81**, 511 (1984).
- ³³H. Jonsson, G. Mills, and K. W. Jacobsen, in *Classical and Quantum Dynamics in Condensed Phase Simulations*, edited by B. J. Berne, G. Ciccotti, and D. F. Coker (World Scientific, Singapore, 1998).
- ³⁴A. Michaelides, V. A. Ranea, P. L. de Andres, and D. A. King, *Phys. Rev. Lett.* **90**, 216102 (2003).
- ³⁵S. Anderson, C. Nyberg, and C. G. Tengstal, *Chem. Phys. Lett.* **104**, 305 (1984).
- ³⁶T. Mitsui, M. K. Rose, E. Fomin, D. F. Ogletree, and M. Salmeron, *Science* **297**, 1850 (2002).
- ³⁷A. D. Rata, A. R. Chezhan, M. W. Haverkort, H. H. Hsieh, H. J. Lin, C. T. Chen, L. H. Tjeng, and T. Hibma, *Phys. Rev. B* **69**, 075404 (2004).
- ³⁸H. Ogasawara, B. Brena, D. Nordlund, M. Nyberg, A. Pelmenchikov, L. G. M. Pettersson, and A. Nilsson, *Phys. Rev. Lett.* **89**, 276102 (2002).
- ³⁹S. Haq, C. Clay, G. R. Darling, G. Zimbitas, and A. Hodgson, *Phys. Rev. B* **73**, 115414 (2006).
- ⁴⁰A. Africh, H. Lin, M. Corso, F. Esch, R. Rosei, W. A. Hofer, and G. Comelli, *J. Am. Chem. Soc.* **127**, 11454 (2005).
- ⁴¹S. Meng, E. G. Wang, and S. W. Gao, *Phys. Rev. B* **69**, 195404 (2004).
- ⁴²S. Meng, L. F. Xu, E. G. Wang, and S. W. Gao, *Phys. Rev. Lett.* **89**, 176104 (2002).
- ⁴³S. Meng, E. G. Wang, Ch. Frischkorn, M. Wolf, and S. W. Gao, *Chem. Phys. Lett.* **402**, 384 (2005).
- ⁴⁴S. Meng, Ph.D. thesis, Chalmers University of Technology, Sweden, 2004.
- ⁴⁵P. Nachtigall, K. D. Jordan, A. Smith, and H. Jonsson, *J. Chem. Phys.* **104**, 148 (1996).
- ⁴⁶S. Meng, *Surf. Sci.* **575**, 300 (2005).
- ⁴⁷E. Schwegler, G. Galli, F. Gygi, and R. Q. Hood, *Phys. Rev. Lett.* **87**, 265501 (2001).
- ⁴⁸P. J. Feibelman, *Phys. Rev. B* **67**, 035420 (2003).
- ⁴⁹D. N. Denzler, Ch. Hess, R. Dudek, S. Wagner, Ch. Frischkorn, M. Wolf, and G. Ertl, *Chem. Phys. Lett.* **376**, 618 (2003).
- ⁵⁰A. Michaelides, A. Alavi, and D. A. King, *J. Am. Chem. Soc.* **125**, 2746 (2003).
- ⁵¹G. Held and D. Menzel, *Phys. Rev. Lett.* **74**, 4221 (1995).
- ⁵²Ch. Frischkorn and M. Wolf (private communication).
- ⁵³J. I. Lee, W. Mannstadt, and A. J. Freeman, *Phys. Rev. B* **59**, 1673 (1999).
- ⁵⁴K.-M. Ho and K. P. Bohnen, *Phys. Rev. Lett.* **59**, 1833 (1987).
- ⁵⁵A. Michaelides, A. Alavi, and D. A. King, *Phys. Rev. B* **69**, 113404 (2004).
- ⁵⁶J. Cerda, A. Michaelides, M.-L. Bocquet, P. J. Feibelman, T. Mitsui, M. Rose, E. Fomin, and M. Salmeron, *Phys. Rev. Lett.* **93**, 116101 (2004).